

# A non-intersecting random walk on the Manhattan lattice and $SLE_6$

Tom Kennedy  
Department of Mathematics  
University of Arizona  
Tucson, AZ 85721  
email: [tgk@math.arizona.edu](mailto:tgk@math.arizona.edu)

May 22, 2018

## Abstract

We consider a random walk on the Manhattan lattice. The walker must follow the orientations of the bonds in this lattice, and the walker is not allowed to visit a site more than once. When both possible steps are allowed, the walker chooses between them with equal probability. The walks generated by this model are known to be related to interfaces for bond percolation on a square lattice. So it is natural to conjecture that the scaling limit is  $SLE_6$ . We test this conjecture with Monte Carlo simulations of the random walk model and find strong support for the conjecture.

## 1 Introduction

There are many different models of random walks on a lattice which generate walks which do not intersect themselves or in which self-intersections are disfavored. In the model that is usually referred to as “the self-avoiding walk”, one considers all nearest neighbor walks of length  $N$  that do not have any self-intersections and defines the probability measure to be the uniform measure on this set of walks. One would then like to let  $N \rightarrow \infty$ . In this model there is not a simple relation between the walks with  $N + 1$  steps and those with  $N$  steps. There are variations on this model. One can consider a bond avoiding random walk in which the walk is allowed to self-intersect, but is not allowed to traverse any bond more than once. Or one can consider a weakly self-avoiding walk in which all nearest neighbors random walks with  $N$  steps are allowed, and the probability of a walk is proportional to  $e^{-\beta I}$  where  $I$  is the number of self-intersections and  $\beta > 0$  is a parameter. See [16] for more on these models. It is conjectured that all these models have the same scaling limit and that the limiting process

is  $\text{SLE}_{8/3}$  [14]. Simulations of the self-avoiding walk support this conjecture [9, 10]. Another model which generates walks with no self intersections is the loop-erased random walk (LERW). One takes an ordinary nearest neighbor random walk on the lattice and erases the loops it forms in chronological order. This model has been proved to converge to  $\text{SLE}_2$  in the scaling limit [15].

In the models above, there is no algorithm that will grow a random walk with the given probability distribution. There is another class of random walks without self-intersections in which the probability measure is defined dynamically, i.e., there is an algorithm that generates a sample of the walk one step at a time. The simplest model is to let the walk choose its next step by randomly picking one of its unoccupied nearest neighbors with equal probability. The problem with this model is that there may not be any unoccupied nearest neighbors; the walk can get trapped. This trapping can be avoided by letting the walk choose any nearest neighbor with probabilities that favor those sites that have not been visited yet. Models of this type are typically called the true self-avoiding walk or the myopic self-avoiding walk [1]. Another model is to let the walk pick with equal probability one of the nearest neighbors that satisfies two conditions - the walk has not visited the neighbor before and there is an infinite path from the neighbor that avoids sites that have been visited before. This model was introduced in the physics literature in the 80's under two names - the smart kinetic walk and the infinitely growing self-avoiding walk [12, 20]. On the hexagonal lattice it is equivalent to the percolation explorer and so is known to have  $\text{SLE}_6$  as its scaling limit. [19, 3]. There is numerical evidence that the scaling limit for the model on the square and triangular lattices is also  $\text{SLE}_6$  [4, 11].

In this paper we study a random walk model on the Manhattan lattice in which the walk is not allowed to visit a site more than once. The Manhattan lattice is an oriented square lattice in which the orientations are constant along horizontal and vertical lines and alternate as we move up or down from a horizontal line or right or left from a vertical line. So if the walk is at  $\omega(n)$  at time  $n$ , there are at most two possibilities for  $\omega(n+1)$ . If both of the possibilities have not been visited before, we randomly choose one with equal probability. If just one possibility has not been visited before,  $\omega(n+1)$  is taken to be that site. If both of the possibilities have been visited before, then the walk will be trapped. It was observed long ago that this can only happen when  $\omega(n)$  is a nearest neighbor of the starting point of the walk [7]. As we will discuss in the next section, this argument also shows that if we restrict the walk to certain domains, the walk will never be trapped. The particular domains we will use for our simulations are a slit plane, the upper right quadrant and the complement of the upper right quadrant.

As we will discuss in the next section, this random walk model is related to interfaces for bond percolation on a square lattice [6]. So a natural conjecture for the scaling limit of this model is  $\text{SLE}_6$ . We will test this conjecture with numerical simulations of the model.

## 2 Definition and equivalent forms of the model

Our model is a random walk on the Manhattan lattice which is not allowed to visit a site more than once. When both possible directions for a step have not been visited before, the walk chooses one with equal probability. If both of the two possible sites for the next step of the walk have been visited before, the walk will be trapped. Hemmer and Hemmer [7] showed that this can only happen when the site is a nearest neighbor of the starting point of the walk. We will repeat their argument.

In figure 1 site  $P$  is the current location of the walk. We assume the walk does not start at  $P_1$  or  $P_2$ . So if  $P_1$  has been visited before, the walk must have followed bond  $b_1$ . And if  $P_2$  has been visited before, the walk must have followed bond  $b_2$ . But this implies that site  $Q$  was visited twice, which is a contradiction.

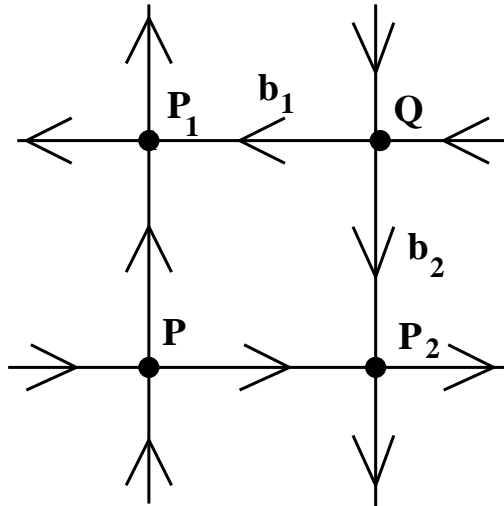


Figure 1: The figure illustrates the argument that the walk cannot get trapped at  $P$ .

Using results from percolation, it can be proved that the walk will return to a nearest neighbor of the starting point and be trapped with probability one [5]. By restricting the walk to certain domains, we can ensure that it will never be trapped. Figure 2 gives three examples. In these figures the walk is not allowed to visit sites on the boundary which is given by the dashed (red) line(s). In the left domain in figure 2, the walk is started at  $P$ . In the right domain, we can start the walk at  $P$  in which case the walk will remain in the upper right quadrant, or we can start it at  $Q$  in which case it will remain in the complement of the upper right quadrant. We will refer to these three domains as the slit plane, the 90 degree wedge and the 270 degree wedge. It is easy to check using arguments similar to the previous paragraph that the walk will never be trapped in these domains with these starting points.

There is an equivalent formulation of the random walk model we have been considering. It uses a different oriented square lattice which is sometimes called the L lattice. The Manhattan

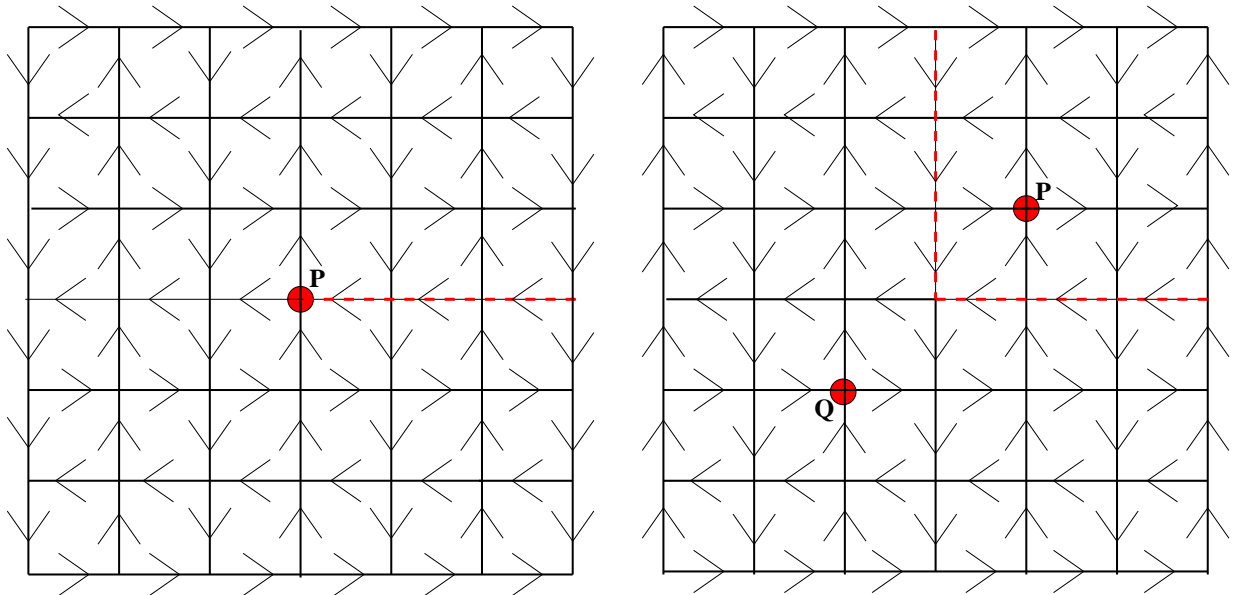


Figure 2: The random walk on the Manhattan lattice with no self-intersections is not allowed to visit sites on the dashed (red) lines. For these three domains, if it starts at  $P$  or  $Q$ , it will never be trapped.

lattice is the “covering lattice” for the L lattice in the sense of Kasteleyn [8]. Figure 3 shows the L lattice and the associated Manhattan lattice. The random walk model on the L lattice is defined as follows. It follows the orientations in the lattice, so at each step it can only turn right or left. It is not allowed to traverse a particular bond more than once, but it can visit a site more than once (but only twice given the bond constraint). When both turns are possible, it chooses between them with equal probability. Given such a random walk on the L lattice, the midpoints of the bonds in the walk will be a walk on the Manhattan lattice that never visits a site in the Manhattan lattice more than once. This gives a 1-1 correspondence between  $n$ -step walks on the L lattice with no repeated bonds and  $(n - 1)$ -step random walks on the Manhattan lattice with no self-intersections. The equivalence of these two random walk models on the Manhattan lattice and the L lattice was observed by Malakis [17].

We note that the term “self-avoiding walk on the Manhattan lattice” is used to refer to the model defined by putting the uniform probability measure on the set of self-avoiding walks on the Manhattan lattice with a fixed number of steps. (For example, [17] considers this model.) This is a completely different model from the model we consider in this paper. We have eschewed the adjective “self-avoiding” for our model to avoid confusion with this other model on the Manhattan lattice.

This random walk on the L lattice that does not repeat bonds can also be formulated as a deterministic random walk in a random environment. This is a special case of the model considered by Gunn and Ortuno [6]. When the random walk makes a turn at a site it has

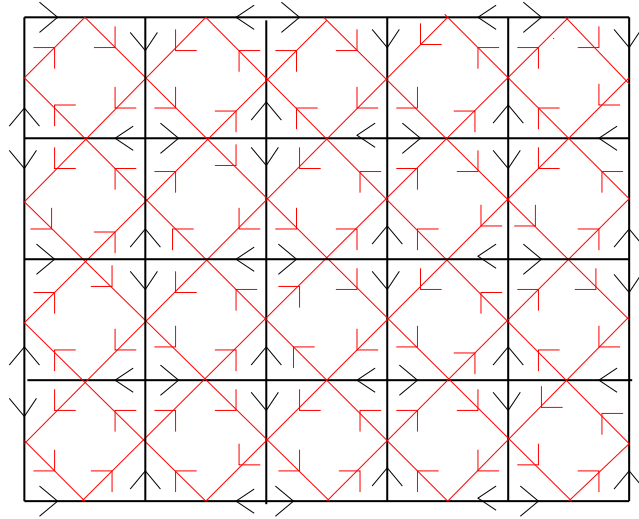


Figure 3: The L lattice is the lattice whose bonds are horizontal and vertical. The associated Manhattan lattice is the (red) lattice whose bonds are at 45 degrees with respect to horizontal and vertical.

not visited before, we place a mirror at that site oriented so that the turn corresponds to the walk being reflected by the mirror. Note that when the walk returns to a site for a second time, the direction of the turn it must make is consistent with the orientation of the mirror that is already at the site. So the mirrors have two possible orientations and they have equal probability. Rather than introduce the mirrors as the walk evolves, we can first randomly place mirrors on all the lattice sites. The walk then evolves in a deterministic manner in this random environment. Note that we must generate a new random environment each time we want to generate a new sample of the random walk.

Finally, we review the relation of the random walk on the L lattice to interfaces in bond percolation on a square lattice. It is worth noting at the start that the bond percolation process does not take place on the L lattice, but rather on a lattice that we will define shortly. The sites in the dual lattice for the L lattice are at the centers of the squares in the L lattice. We take the length of the mirrors to be  $\sqrt{2}$ . (The lattice spacing is 1.) Then the ends of the mirrors are at sites in the dual lattice which are next nearest neighbors. The dual lattice is a bipartite lattice, i.e., we can label the sites in the dual lattice as even or odd in such a way that an odd site has only even sites as its nearest neighbors and vice versa. So the ends of the mirrors will either be both odd or both even. Hence we can label the mirrors as even or odd. If we just consider the even sites in the dual lattice, we have a square lattice with spacing  $\sqrt{2}$ , rotated by 45 degrees with respect to the dual lattice. We will refer to this lattice as the even half-dual lattice. The odd half-dual lattice is defined similarly. The even mirrors are bonds in the even half-dual lattice, and the odd mirrors are bonds in the odd half-dual lattice. Note that each site in the L lattice is the midpoint of one bond in the even half-dual lattice and one bond in

the odd half-dual lattice. There is a mirror at every site in the L lattice, and it will be the odd bond with probability  $1/2$  or the even bond with probability  $1/2$ . So the even mirrors have the distribution of bond percolation on the even half-dual lattice. Likewise, the odd mirrors have the distribution of bond percolation on the odd half-dual lattice. These two percolations processes are not independent. In fact, the configuration of odd mirrors completely determines the configuration of the even mirrors and vice versa.

Gunn and Ortuno [6] showed that the random walk on the L lattice is sandwiched between a connected cluster for the bond percolation on the odd half-dual lattice and a connected cluster for the bond percolation on the even half-dual lattice. Figure 4 shows a section of a random walk. Only the mirrors that touch the random walk are shown. As one traverses the random walk, one of the connected clusters is always on the right and the other is always on the left. So we can think of the random walk as either tracing out an interface for the bond percolation process on the even half-dual lattice or an interface for the bond percolation process on the odd half-dual lattice. Since our random walk on the Manhattan lattice with no self-intersections is equivalent to the random walk on the L lattice with no repeated bonds, the random walk on the Manhattan lattice is also related to interfaces in bond percolation on the square lattice. This relation was described in [2]. Ziff, Cummings and Stells studied other random walk models that are related to percolation interfaces [22].

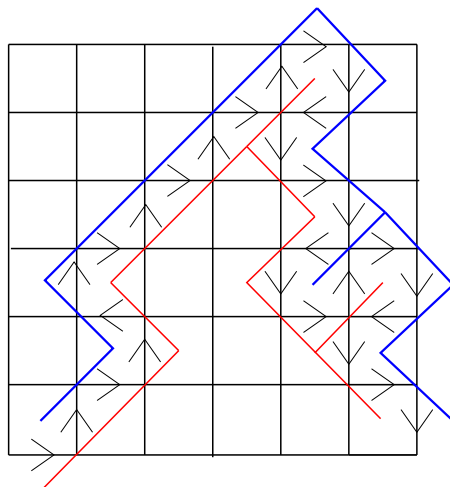


Figure 4: A portion of a random walk on the L lattice is shown with arrows. It is sandwiched between a connected component of even mirrors and a connected component of odd mirrors.

### 3 Tests for $\text{SLE}_6$

#### 3.1 Hitting distribution

We test the conjecture that the scaling limit is  $\text{SLE}_6$  by studying two quantities that can be computed explicitly for  $\text{SLE}_6$ . The first quantity is a type of hitting distribution. We first consider our model in the left domain in figure 2, i.e., the plane slit along the positive real axis. We consider a circle of radius  $r$  and stop the random walk when it first hits this circle. The random variable we study is the polar angle of the point where the walk first hits the circle. The distribution of this random variable for  $\text{SLE}_6$  is known explicitly.

Our walk is going from 0 to  $\infty$ , so in the scaling limit our conjecture is that we get  $\text{SLE}_6$  in the slit plane going from 0 to  $\infty$ . We will refer to the subset of the slit plane with  $|z| < r$  as the slit disc. Because of the locality property of  $\text{SLE}_6$ , up until the time the  $\text{SLE}_6$  curve hits the circle of radius  $r$ , the distribution of the curve is the same as that of an  $\text{SLE}_6$  curve in the slit disc going from 0 to any fixed point on the circle. Note that each point on the positive real axis is really two boundary points for the slit plane, one as we approach the axis from above and one as we approach it from below. We distinguish the two boundary points that correspond to an  $x > 0$  by  $x^+$  and  $x^-$ . We take the terminal point for the  $\text{SLE}_6$  to be  $r^-$ . So we consider  $\text{SLE}_6$  in the slit disc with radius  $r$  starting at 0 and ending at  $r^-$  and want to know the distribution of the first point where it hits the circle of radius  $r$ . We take the conformal map of the slit disc to the half plane which sends 0 to 0,  $r^-$  to  $\infty$  and  $r^+$  to 1. The boundary of the slit disc is mapped to the real axis, and the part of the boundary of the slit disc that is the circle of radius  $r$  is mapped to  $[1, \infty)$ . So we can find the distribution of the hitting point for the circle of radius  $r$  if we can find the distribution of where  $\text{SLE}_6$  in the half plane first hits  $[1, \infty)$ .

This distribution is known. For  $\kappa > 4$ , the SLE curve will touch the real axis infinitely often. Let  $\gamma(t)$  denote the SLE trace, and let  $t^*$  be the first time it touches the subset  $[1, \infty)$  of the real axis. So  $\gamma(t^*)$  is the place it first hits  $[1, \infty)$ . Its distribution is the following; see proposition 6.34 in [13].

$$P(\gamma(t_*) < 1 + x) = cI\left(\frac{x}{x+1}\right), \quad (1)$$

$$I(x) = \int_0^x u^{-2/3}(1-u)^{-2/3} du \quad (2)$$

with  $c = 1/I(1)$ .

Returning to our walk in the slit disc, the conformal map of the slit disc to the half plane which sends 0 to 0,  $r^-$  to  $\infty$  and  $r^+$  to 1 can be constructed as follows. We take  $r = 1$ . Define

$$\phi(z) = \frac{1}{2}\left(z + \frac{1}{z}\right), \quad \psi(z) = \frac{2}{1+z} \quad (3)$$

First we apply the map  $z \rightarrow \sqrt{z}$  to map the slit disc to the half disc in the upper half plane. Then we apply the map  $\phi(z)$  to map this half disc to the half plane below the real axis. Finally

we apply the Moibius transformation  $\psi(z)$  to get the points  $0$ ,  $r^+$  and  $r^-$  to go to the appropriate points. So the overall conformal map is given by  $\psi(\phi(\sqrt{z}))$ . We have

$$\psi(\phi(\sqrt{Re^{i\theta}})) = 1 + x, \quad x = \frac{1 - \cos(\theta/2)}{1 + \cos(\theta/2)} \quad (4)$$

and so the cumulative distribution function (CDF) for the hitting distribution of the walk in the half plane is  $F(\theta) = cI(x)$  with  $x$  given above.

For the 90 degree wedge, the conformal map  $z \rightarrow z^4$  maps the region to the slit plane, so the CDF is given by the above with the only change being that we replace  $\theta$  by  $4\theta$  in the definition of  $x$ . For our 270 degree wedge, the polar angle ranges from  $\pi/2$  to  $2\pi$ . The only change we need to make in the above is to replace  $\theta$  in the definition of  $x$  by  $\frac{4}{3}(\theta - \pi/2)$ .

Since we are looking at the first time that the walk hits a circle of radius  $R$ , we need only simulate the walk up until the time it hits the circle. Unlike the next test that we will consider, we do not need to worry about the limit of taking the number of steps in the walk to infinity. The simulations will be done with a lattice spacing of 1, so  $\delta = 1/R$  can be thought of as the effective lattice spacing. The scaling limit is given by letting  $\delta \rightarrow 0$ , i.e.,  $R \rightarrow \infty$ .

Before we take the scaling limit, the random variable we are studying is discrete; there are only a finite number of points where the walk can first hit the circle. Of course, in the scaling limit it should converge to a continuous random variable. The discreteness of the random variable will be quite visible in our simulation results. We can reduce the effect of this discreteness in the following way. As the radius  $R$  changes, the set of possible values of the discrete random variable changes. So if we average the random variable over an interval of radii  $R$ , we get a continuous random variable. We will refer to this as ‘‘averaging over  $R$ .’’ So if we let  $\Theta_R$  denote that random variable for a circle of radius  $R$ , then we consider instead the averaged random variable

$$\Theta_{R_0, R_1} = \frac{1}{R_1 - R_0} \int_{R_0}^{R_1} \Theta_r dr \quad (5)$$

We will always take  $R_0 = R, R_1 = 2R$ . So the scaling limit is given by taking  $R \rightarrow \infty$ . Obviously, the distribution of the limit of  $\Theta_{R, 2R}$  should be the same as the distribution of the limit of  $\Theta_R$ .

## 3.2 Pass right function

The other quantity we study is the following. Let  $z_0$  be a point in the domain where the walk is taking place. We consider the probability that the SLE trace passes to the right of the point. Since the SLE trace has self-intersection points (as does the random walk), the definition of passing right of a point is not completely obvious. It can be defined using winding numbers as in [18]. A more practical definition for computational purposes is the following. Given the SLE curve (or a random walk), take a curve from  $z_0$  to a point on the positive real axis which is



generic in the sense that it does not pass through any self-intersection points of the SLE curve (or the random walk). Count the number of intersections of this curve with the SLE curve (or the random walk). If this number is odd, the SLE curve (or random walk) passes right of  $z_0$ , if even it passes left.

Schramm derived an explicit formula for this probability for  $SLE_\kappa$  [18]. In domains such as the half-plane, the slit-plane or the wedges we consider, by the dilation invariance of SLE this probability only depends on the polar angle of the point. We will refer to this probability of passing right of a point with polar angle  $\theta$  as the pass-right function and denote it by  $p_{SLE}(\theta)$ . In the half plane, Schramm's formula is

$$p_{SLE}(\theta) = c \int_0^\theta [\sin(t)]^{-2+8/\kappa} dt \quad (6)$$

where the constant  $c$  is defined by  $p(\pi) = 1$ . The half plane is mapped onto our three domains by a map of the form  $z \rightarrow z^p$ , so the formula for our domains is given by replacing  $\theta$  in the right side by  $\theta/2$  for the slit plane, by  $2\theta$  for the 90 degree wedge and by  $\frac{2}{3}(\theta - \pi/2)$  for the 270 degree wedge.

In our simulations we will compute the probability of passing right of  $Re^{i\theta}$  with  $R$  fixed and  $\theta$  varying. We denote this probability by  $p_R(\theta)$ . If the scaling limit of our random walk is  $SLE_6$ ,  $p_R(\theta)$  should converge to  $p_{SLE}(\theta)$  as  $R \rightarrow \infty$ .

Note that there is not a natural time at which we should stop the generation of the walk when we study the probability of passing right. No matter how far the walk is outside the circle of radius  $R$ , there is always some probability that the walk will cross this circle again and so change whether some points on the circle are right or left of the walk. Unlike the first test we considered, we need to let the number of steps in the walk go to  $\infty$ . The simulation uses a lattice of spacing 1. If we rescale so that the circle has radius 1, then the lattice spacing becomes  $1/R$ . So we will refer to  $\delta = 1/R$  as the lattice spacing. Note that how "close"  $N$  is to infinity depends on  $R$ . The number of steps it takes the walk to first reach the circle of radius  $R$  is of order  $R^{1/\nu}$ . (We take  $\nu = 4/7$ .) So we define  $n = N/R^{1/\nu}$ . The proper way to measure how large  $N$  is, is to consider how large  $n$  is with respect to 1. We now must take a double limit to obtain the scaling limit;  $\delta$  must go to zero and  $n$  must go to  $\infty$ .

For finite  $R$ , the function  $p_R(\theta)$  is a step function since there are only a finite number of points where the walk can cross the circle of radius. As with the previous random variable, we can smooth out this function by averaging  $R$  over some interval. So we define

$$p_{R_0, R_1}(\theta) = \frac{1}{R_1 - R_0} \int_{R_0}^{R_1} p_r(\theta) dr \quad (7)$$

We will always take  $R_0 = R, R_1 = 2R$ . So if we define  $n = N/R^{1/\nu}$ , then the scaling limit is given by letting  $R$  go to  $\infty$  and  $n$  go to  $\infty$ .

## 4 Simulation results

### 4.1 Hitting distribution

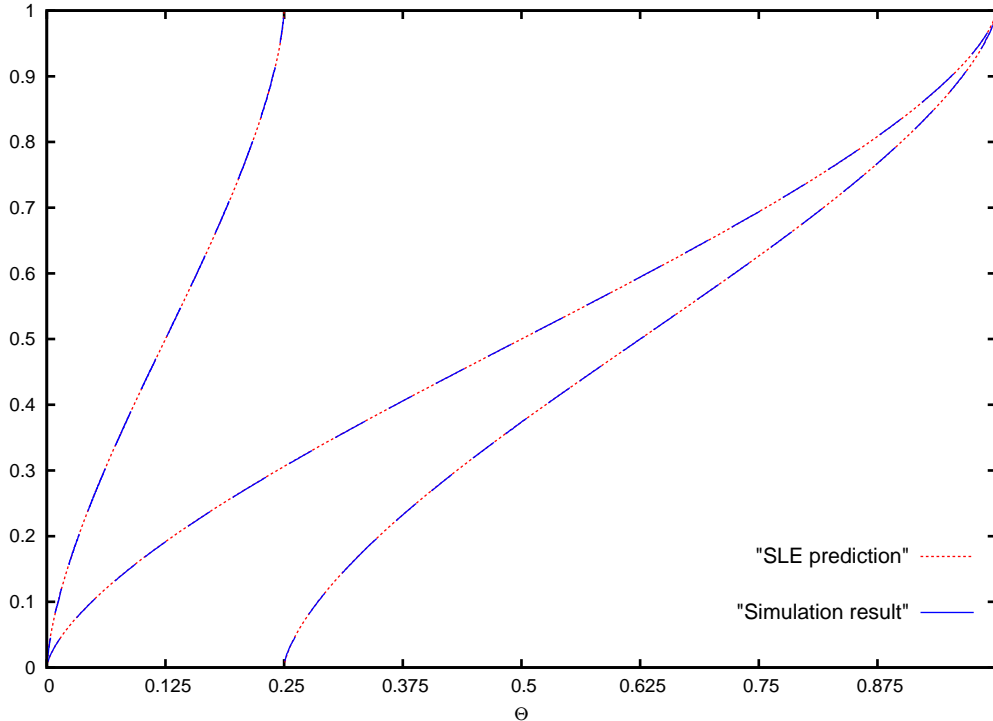


Figure 5: Comparison of the CDF for the hitting distribution for the random walk and  $SLE_6$  for three domains. The two curves for the slit plane have  $\Theta \in [0, 1]$ , for the 90 degree wedge  $\Theta \in [0, 1/4]$  and for the 270 degree wedge  $\Theta \in [1/4, 1]$ .

We first consider the hitting distribution for three domains - the slit plane, the 90 degree wedge and the 270 degree wedge. Recall that by the hitting distribution we mean the polar angle of the point where the walk first hits a circle of radius  $R$ . The scaling limit is taken by letting  $R \rightarrow \infty$ . In all our figures the variable  $\Theta$  is actually the polar angle divided by  $2\pi$ . So it runs from 0 to 1 for the slit plane, from 0 to  $1/4$  for the 90 degree wedge and from  $1/4$  to 1 for the 270 degree wedge. In figure 5 we plot the CDF for this hitting distribution for the three domains. For each domain two CDF's are plotted - the simulation CDF and the CDF predicted by  $SLE_6$ . They agree so well that the curves cannot be distinguished. We plot only "half" of each curve so that the overlapping curves can be seen. The simulations shown used a radius of  $R = 800$ .

In figure 6 we plot the difference between the simulation CDF and the  $SLE_6$  CDF for the hitting distribution for the slit plane for radii of 200, 400, 800. One sees that the difference is getting smaller as  $R$  gets larger. The sawtooth nature of these plots can be understood as

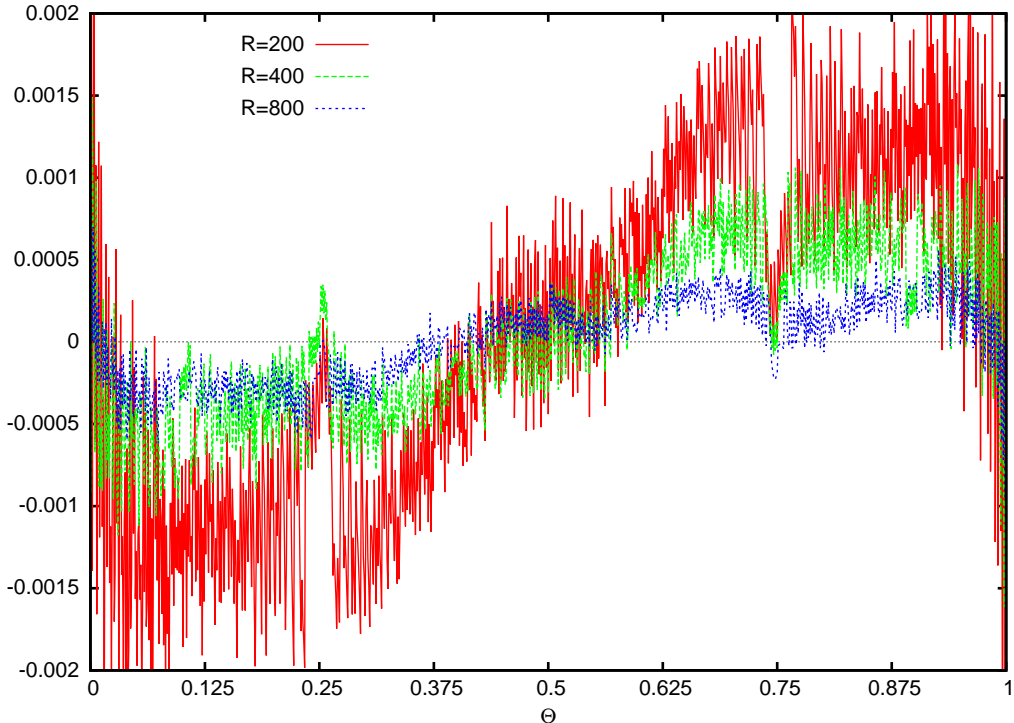


Figure 6: The difference of the CDF's for the hitting distribution for the random walk and  $SLE_6$  for the slit plane. The three curves are for  $R = 200, 400, 800$  to study the limit of the lattice spacing going to zero, i.e.,  $R \rightarrow \infty$ .

follows. In the simulation the random variable being studied is discrete. So its CDF is a step function. When we subtract the smooth CDF from  $SLE_6$  we get a sawtooth effect. As the radius gets larger this lattice effect gets smaller.

As discussed in the previous section, we can reduce this lattice effect by averaging over  $R$ . Figure 7 shows the effect of this averaging. There are two plots of the difference between the simulation CDF and the  $SLE_6$  CDF. The sawtooth curve is for  $R = 375$  without averaging. For the other curve  $R$  is averaged over  $[250, 500]$ . This plot shows that the averaging greatly reduces the sawtooth effect. Note that the overall magnitude of the difference is not reduced by this averaging. The averaging smooths out the discreteness of the random variable, but we still need to let the endpoints of the interval over which we average go to infinity to take the scaling limit.

In figure 8 we plot the difference between the simulation CDF and the  $SLE_6$  CDF for the hitting distribution for the slit plane with this averaging. The intervals over which the radius  $R$  is averaged are  $[125, 250]$ ,  $[250, 500]$ ,  $[500, 1000]$ ,  $[1000, 2000]$ . In figures 9 and 10 we show the analogous plots for the 90 degree wedge and the 270 degree wedge. In these plots the error bars shown represent plus/minus two standard deviations for the statistical errors that are a result

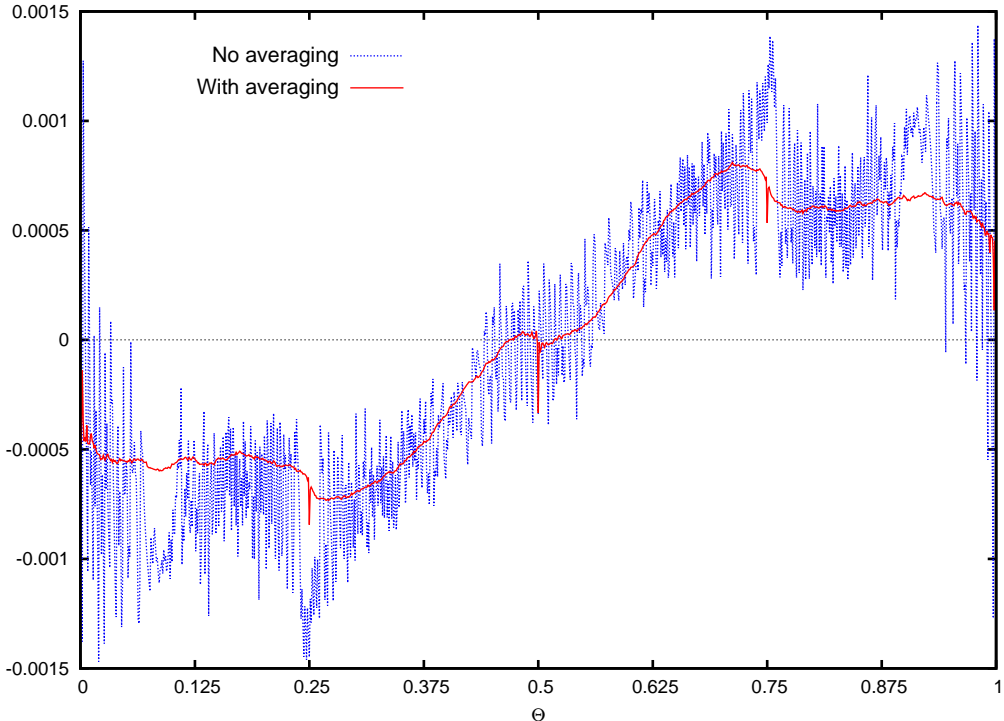


Figure 7: The effect of averaging on the difference between the hitting distributions for the random walk and  $\text{SLE}_6$  in the slit plane. The highly oscillatory (blue) curve is for  $R = 375$ . The smoother solid (red) curve averages  $R$  over  $[250, 500]$ .

of the number of samples being finite. The error bars do not represent the error that comes from not having completely converged to the scaling limit. In all three figures the difference can be seen to decrease as  $R$  increases and is quite small. (Note the scale on the vertical axis.) For the largest value of  $R$  the size of the difference is comparable to the statistical errors.

## 4.2 Pass right function

We now study the probability of passing right of a point  $Re^{i\theta}$  as a function of the polar angle  $\theta$ . As discussed before,  $\delta = 1/R$  is the effective lattice spacing and  $n = N/R^{1/\nu}$  is the effective length of the walk (compared to the number of steps needed to reach the circle for the first time). To obtain the scaling limit we must let  $\delta$  go to zero and  $n$  to  $\infty$ . Since we average  $R$  over an interval, both  $\delta$  and  $n$  vary over an interval in each simulation. When we give explicit values for  $\delta$  and  $n$ , we will compute them using the midpoint of the interval for  $R$ .

If we generate samples of walks with  $N$  steps, then we can use these samples as samples of walks with  $fN$  steps for  $f < 1$ . (We do this for the sake of efficiency.) So in our simulations we have three parameters:  $N_0$ ,  $f$  and  $r$ .  $N_0$  is the number of steps in the walks being generated, while  $N = fN_0$  is the number of steps that we actually use. The radius  $R$  is taken to be

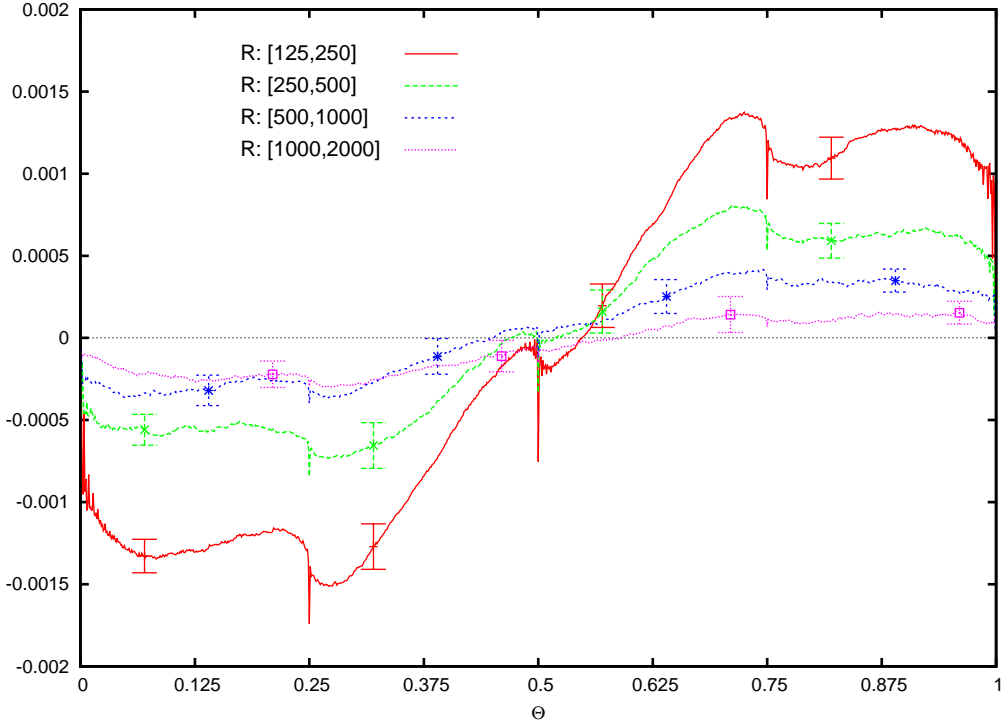


Figure 8: The difference of the hitting distributions for the random walk and  $SLE_6$  for the slit plane.  $R$  is averaged over four different intervals to study the limit of the lattice spacing going to zero, i.e.,  $R \rightarrow \infty$ .

$R = rN_0^\nu$ . So the effective lattice spacing  $\delta$  and the length of the walk  $n$  are given in terms of  $N_0, f$  and  $r$  by

$$\delta = \frac{1}{rN_0^\nu}, \quad n = \frac{fN_0}{r^{1/\nu}N_0} = \frac{f}{r^{1/\nu}} \quad (8)$$

To study the probability of passing right we use the averaging trick described before. In figure 11 we plot the pass right function with  $r$  averaged over  $[0.05, 0.1]$  and this function with  $r = 0.075$ . For both of these plots  $N = 125K$ . We also plot the  $SLE_6$  prediction. Without averaging the CDF has large oscillations. The averaging removes these oscillations and the averaged CDF is centered in the middle of the oscillations. However, the averaged CDF does not agree at all with the  $SLE_6$  CDF. The difference between the two curves is as large as 5% for some  $\theta$ .

The large discrepancy between the simulation and the  $SLE_6$  prediction could be the result of the lattice spacing  $\delta$  not being sufficiently small or the result of the length of the walk  $n$  not being sufficiently large (or both). As we will show, it is primarily the result of  $n$  not being sufficiently large. We first show that the effect of the lattice spacing  $\delta$  on this large discrepancy is negligible. Figure 12 shows two differences. Both differences use  $r = 0.1$  and  $f = 1$ . One

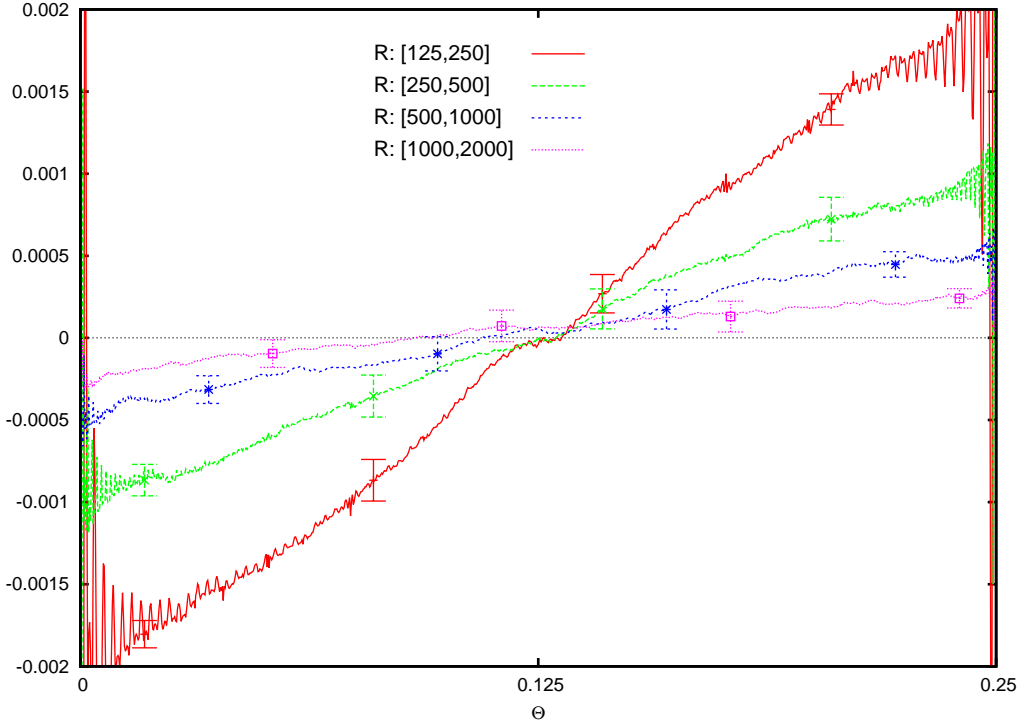


Figure 9: The difference of the hitting distributions for the random walk and  $SLE_6$  for the 90 degree wedge.  $R$  is averaged over four different intervals to study the limit of the lattice spacing going to zero, i.e.,  $R \rightarrow \infty$ .

difference uses  $N_0 = 125K$  and the other  $N_0 = 1000K$ . So the length of the walk  $n$  is the same for the two differences. The effective lattice spacings are given by  $\delta = 1/(rN_0)^p$  which takes on the values 0.0163 and 0.00497. So  $\delta$  varies by a factor of  $8^{4/7} \approx 3.3$ , but the figure shows that the difference hardly changes. In this figure and the remaining figures in the paper we do not show any error bars since they are tiny compared to the differences plotted in these figures. Two standard deviations are on the order of  $10^{-4}$  which is much smaller than the vertical scale of the plots in figures 12 to 18.

Next we fix  $\delta$  and vary  $n$ . We do this by fixing  $N_0 = 10^6$  and fixing the interval  $r$  over which we average to be  $[0.05, 0.10]$ . Then we vary  $f$  over  $1/8, 1/4, 1/2, 1$ . So in all four cases the lattice spacing  $\delta$  is averaged over the same interval while the length of the walk  $n$  is averaged over four different intervals. We use the midpoint of the interval for  $R$  to compute explicit values for  $n$ . They are  $n = 11.6, 23.3, 46.5, 93.0$ . The resulting four differences are shown in figure 13 for the slit plane. The difference looks like it is going to zero as  $n$  goes to infinity, and by studying the size of these curves it appears it is converging as  $n^{-p}$  where a crude estimate of  $p$  is 0.24.

We test this by rescaling the difference curves with a factor proportional to  $n^p$ . The curve

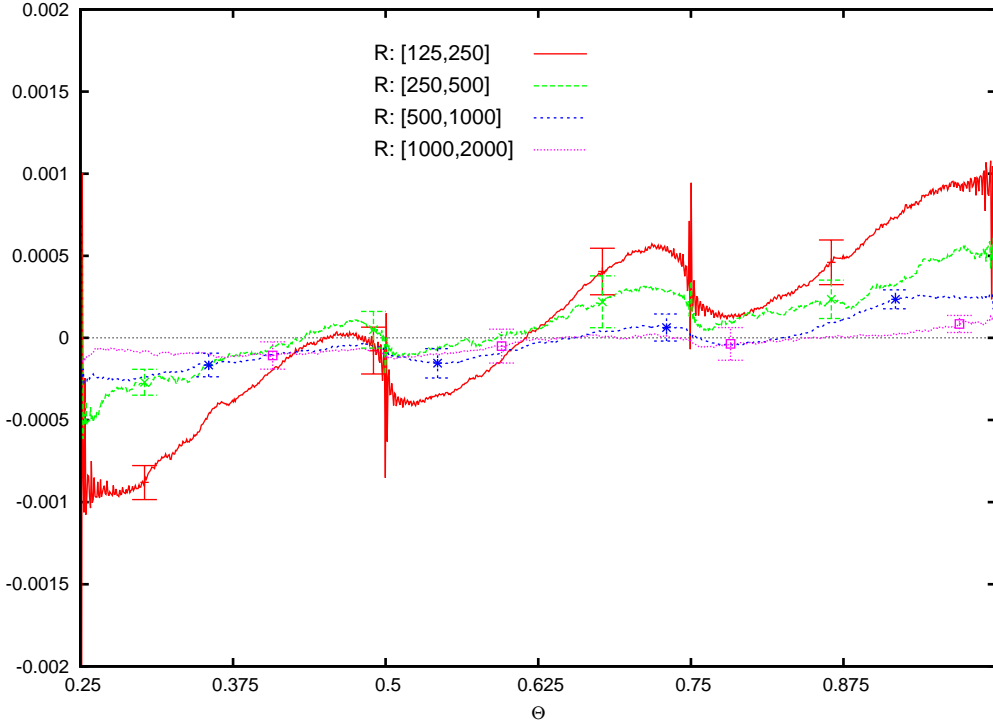


Figure 10: The difference of the hitting distributions for the random walk and  $SLE_6$  for the 270 degree wedge.  $R$  is averaged over four different intervals to study the limit of the lattice spacing going to zero, i.e.,  $R \rightarrow \infty$ .

for  $n = 93.0$  is rescaled by a factor of  $2^{3p}$ , the curve for  $n = 46.5$  by a factor of  $2^{2p}$  and the curve for  $n = 23.3$  by a factor of  $2^p$ . The curve for  $n = 11.6$  is not rescaled. These rescaled curves are shown in figure 14 for  $p = 0.24$ . They agree well. Note that all four differences in figure 13 use the same non-zero lattice spacing. So we do not expect them to converge exactly to zero. So we expect the rescaled differences in figure 14 to differ slightly.

In figure 15 we plot the difference for the 90 degree wedge with  $\delta$  fixed and  $n$  varying just as we did for the slit plane. (We take  $N_0 = 10^6$ , average  $r$  over  $[0.05, 0.10]$ , and vary  $f$  over  $1/8, 1/4, 1/2, 1$ .) For the 90 degree wedge the difference converges to zero much faster as  $n$  goes to infinity. Again, the convergence appears to go as  $n^{-p}$ , but now a crude estimate of  $p$  gives the much larger value of 1.15. In figure 16 we rescale these differences by a factor proportional to  $n^p$  just as we did for the slit plane. The rescaled curves agree well. The lattice effects appear larger here compared to the slit plane because the rescaling factors of  $2^p, 2^{2p}$  and  $2^{3p}$  are considerably larger than for the slit plane.

While the simulations provide strong evidence that in the scaling limit the pass right function for the random walk is converging to the  $SLE_6$  prediction, the slow convergence of the  $n \rightarrow \infty$  limit, especially for the slit plane, is rather surprising. So it is instructive to look at the

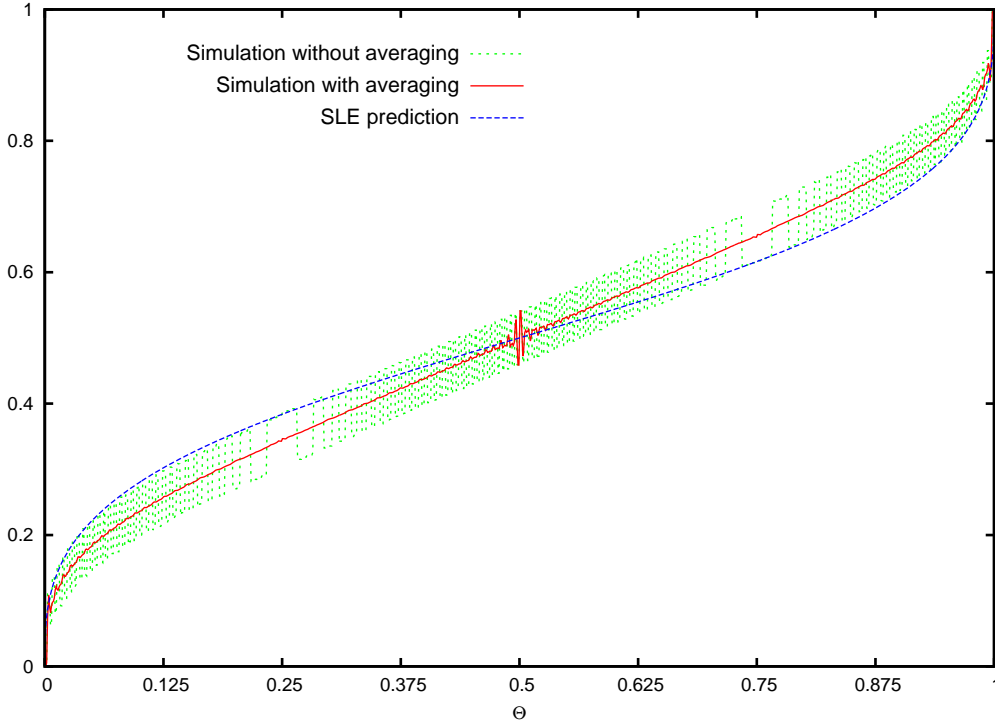


Figure 11: The pass right function for the random walk and  $SLE_6$ . The highly oscillatory (green) curve is the random walk without averaging. The solid (red) curve which passes through the center of the oscillatory curve is for the random walk with averaging. The dashed (blue) curve is for  $SLE_6$ .

analogous simulation for the percolation explorer on the hexagonal lattice which is proven to converge to  $SLE_6$ . We give a brief description of this model and refer the reader to [21] for more detail. We work in the half-plane. The hexagons above the horizontal axis are randomly colored black or white with equal probability. The hexagons along the horizontal axis that are to the right of the origin are colored white, and those to the left of the origin are colored black. We now consider the interfaces between black and white hexagons. These interfaces will form loops with one exception. The choice of boundary condition forces there to be an interface which starts at the origin and is of infinite length. This random curve is the percolation explorer which has been proved to converge to  $SLE_6$ . We have simulated this percolation explorer and computed the probability of passing right of the points along a circle just as we did for our random walk model. We have used the same parameters (and hence the same  $\delta$  and  $n$  values) that we did for the random walk model. In figure 17 we plot the difference between the simulation CDF and the  $SLE_6$  CDF for the slit plane. So this figure is the analog of figure 13. The difference curves from the percolation simulation are remarkably similar to the difference curves from our random walk simulations.

Just as in figure 13 we see that the difference is large, but appears to be going to zero.



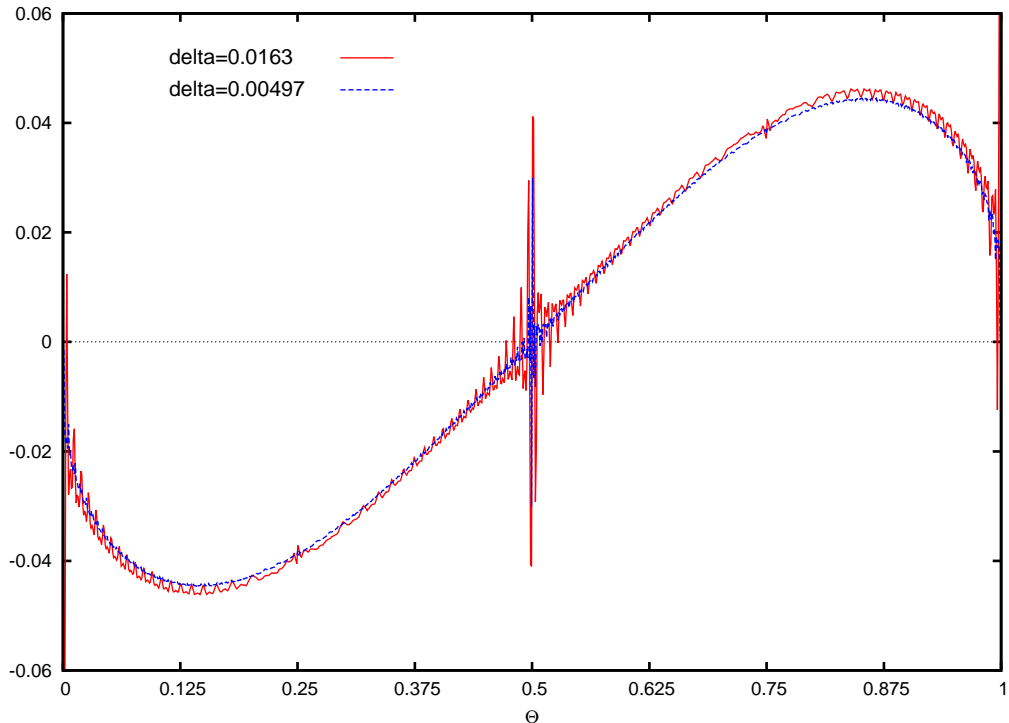


Figure 12: The difference between the random walk and  $\text{SLE}_6$  pass right functions for the slit plane when the length  $n$  of the walk is kept fixed and the lattice spacing  $\delta$  is varied.

We can check this more carefully by rescaling. Figure 18 shows the rescaled differences for percolation, so this figure is the analog of figure 14. We use the same power  $p = 0.24$  that we used for the random walk model.

### 4.3 Details of the simulation

The algorithm to generate the walk is very simple. At each step we must determine which of the two possible steps are not allowed, i.e., which of these two sites have been visited before or belong to the boundary. We check if they have been visited before using a hash table. If both sites have not been visited and are not on the boundary, we randomly choose between them with equal probability.

The time to generate a walk is proportional to the number of steps. Some care is needed to be sure the time it takes to evaluate the pass right function does not dominate the computation time. In particular, computing the intergral involved in our averaging for each random walk sample would be prohibitively expensive. Instead, we incorporate the evaluation of this integral into the Monte Carlo simulation. For each sample of the random walk we randomly choose an  $R$  uniformly from  $[R_0, R_1]$  and just compute the pass right function or the hitting point for that radius  $R$ .

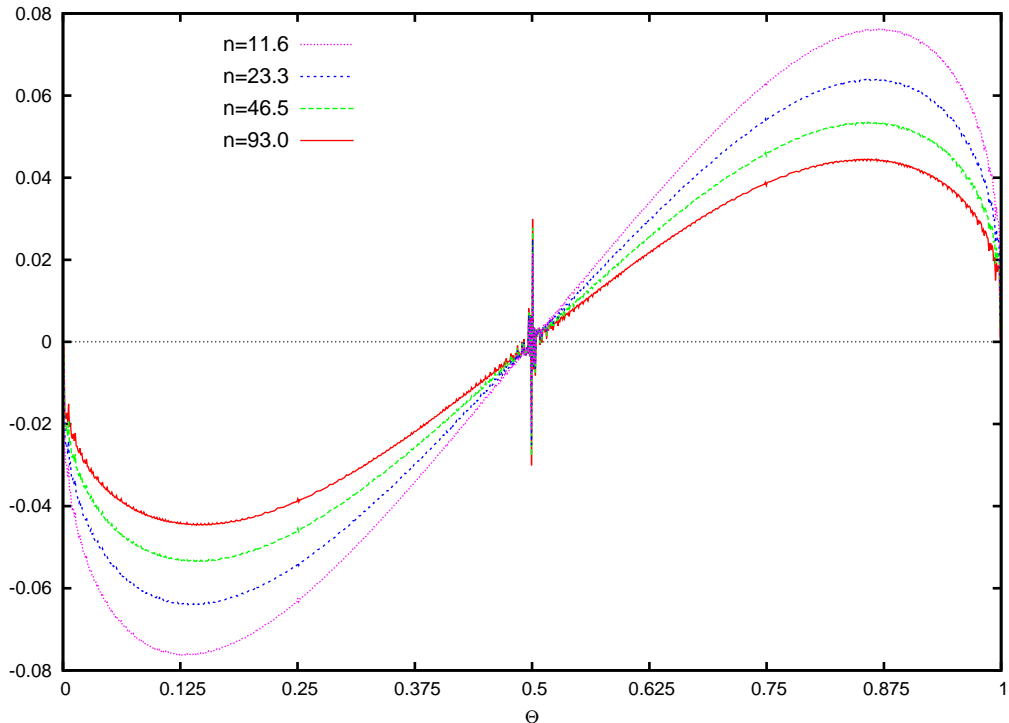


Figure 13: The difference between the random walk and  $SLE_6$  pass right functions for the slit plane when the lattice spacing  $\delta$  is kept fixed and the length  $n$  of the walk is varied.

In all our simulations we generate  $10^8$  samples of the random walk. The time needed depends on the domain and the parameters which control the number of steps in the walk. Furthermore, these computations are done on a large cluster with many users. So we only have a crude estimate of the CPU time used. The longest simulations take roughly on the order of 200 CPU-days to generate  $10^8$  samples.

## 5 Conclusions

We have studied a random walk model on the Manhattan lattice which is not allowed to visit a site more than once. This model is known to be related to interfaces for bond percolation on a square lattice, so it is natural to conjecture that its scaling limit should be  $SLE_6$ . We have tested this conjecture with Monte Carlo simulations of two quantities. One is a sort of hitting distribution. The other is the probability of passing to the right of a given point.

For the hitting distribution we found excellent agreement with the  $SLE_6$  prediction for this quantity. For the domains we consider, the scaling limit of the probability of passing right requires taking a double limit - letting the lattice spacing go to zero and the length of the walk to infinity. The convergence for the latter is surprisingly slow and there are significant

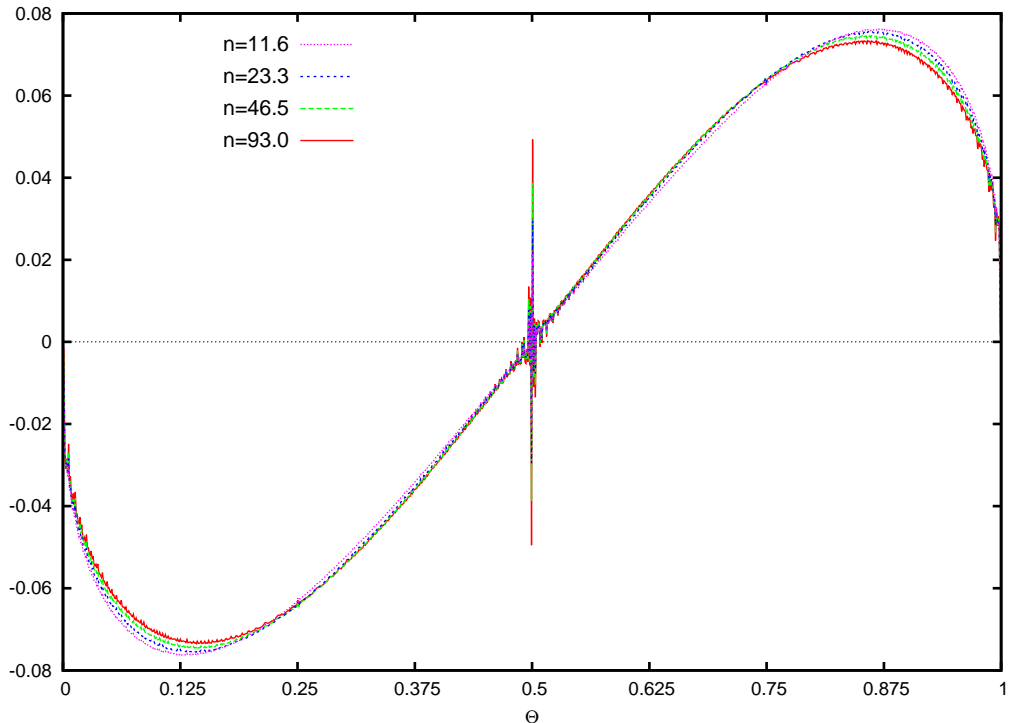


Figure 14: The same differences shown in the previous plot are replotted but multiplied by a factor proportional to  $n^p$  with  $p = 0.24$  to test if the differences in the previous plot are proportional to  $n^{-p}$ .

differences between the function we find in our simulations and the  $\text{SLE}_6$  prediction for this function. However, we can fit the difference quite well by a function proportional to  $n^{-p}$  where  $n$  is the length of the walk. Moreover, the differences we see in our model are remarkably similar to the analogous differences for the percolation explorer on the hexagonal lattice which been proven to converge to  $\text{SLE}_6$ . We conclude that our simulations provide strong support for the conjecture that the scaling limit of the random walk on the Manhattan lattice with no self-intersections is  $\text{SLE}_6$ .

*Acknowledgments:* This research was supported in part by NSF grant DMS-1500850. An allocation of computer time from the UA Research Computing High Performance Computing (HPC) and High Throughput Computing (HTC) at the University of Arizona is gratefully acknowledged.

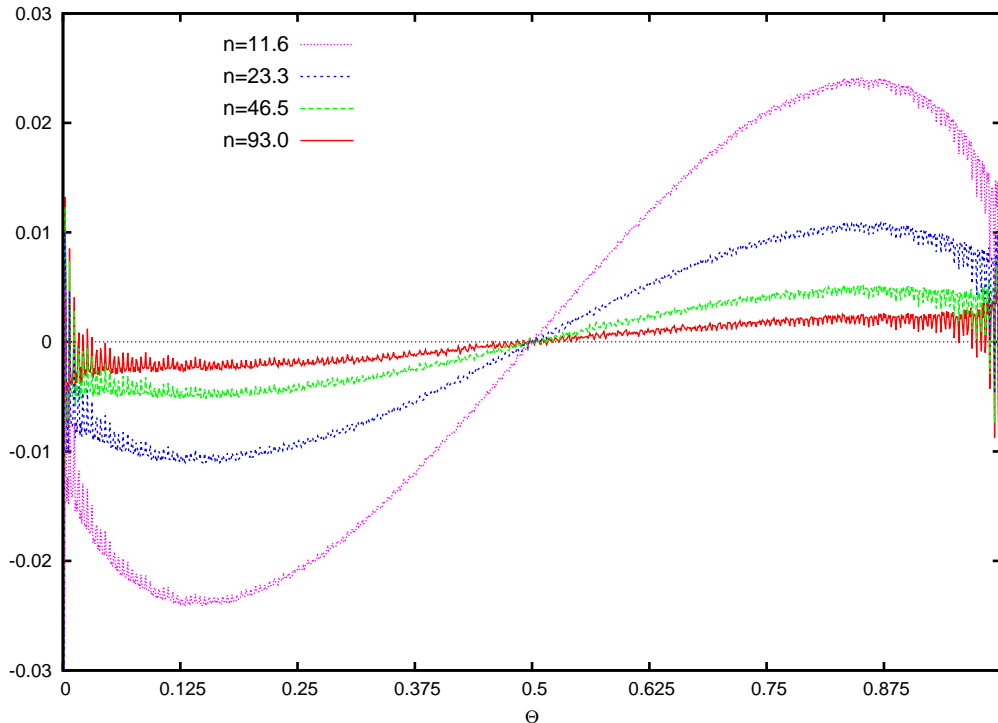


Figure 15: The difference between the random walk and  $SLE_6$  pass right functions for the 90 degree wedge when the lattice spacing  $\delta$  is kept fixed and the length  $n$  of the walk is varied.

## References

- [1] D. J. Amit, G. Parisi, L. Peliti, Asymptotic behavior of the “true” self-avoiding walk. *Phys. Rev. B* **27**, 1635 (1983).
- [2] R. M. Bradley, Exact  $\theta$  point and exponents for polymer chains on an oriented two-dimensional lattice. *Phys. Rev. A* **39** 3738–3740 (1989).
- [3] F. Camia, C. M. Newman, Critical percolation exploration path and  $SLE_6$  : a proof of convergence. *Probab. Theory Related Fields* **139**,473–519 (2007). Archived as arXiv:math/0605035 [math.PR].
- [4] Y. Dai, The Exit Distribution for smart kinetic walk with symmetric and asymmetric transition probability, *J. Stat. Phys.* **166**, 1455-1463 (2017). Archived as arXiv:1611.09779[math.PR].
- [5] G. Grimmett, *Percolation*, Springer (1999).
- [6] J. M. F. Gunn, M. Ortuno, Percolation and motion in a simple random environment. *J. Phys. A* **18**, L1095 (1985).

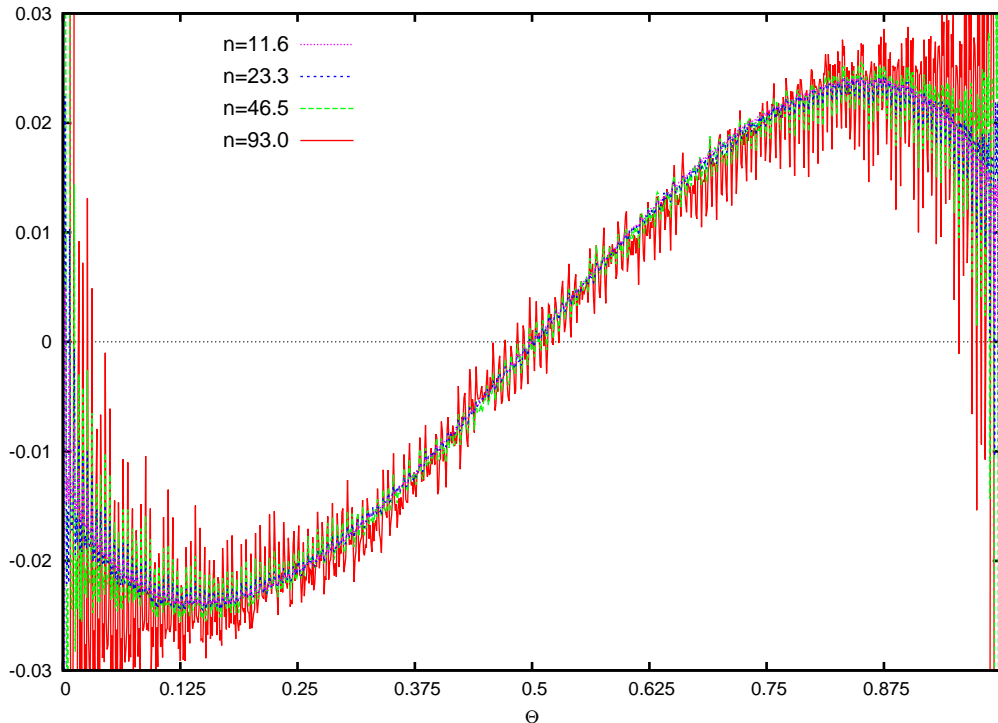


Figure 16: The same differences shown in the previous plot are replotted but multiplied by a factor proportional to  $n^p$  with  $p = 1.15$  to test if the differences in the previous plot are proportional to  $n^{-p}$ .

- [7] P. C. Hemmer, S. Hemmer, Trapping of genuine self-avoiding walks, *Phys. Rev. A* **34**, 3304 (1986).
- [8] P. W. Kasteleyn, A soluble self-avoiding walk problem. *Physica* **29** 1329-1337 (1963).
- [9] T. Kennedy, Monte Carlo tests of SLE predictions for 2D self-avoiding walks. *Phys. Rev. Lett.* **88**, 130601 (2002). Archived as arXiv:math/0112246v1 [math.PR].
- [10] T. Kennedy, Conformal invariance and stochastic Loewner evolution predictions for the 2D self-avoiding walk - Monte Carlo tests. *J. Stat. Phys.* **114**, 51-78 (2004). Archived as arXiv:math/0207231v2 [math.PR].
- [11] T. Kennedy, The smart kinetic self-avoiding walk and Schramm-Loewner evolution. *J. Stat. Phys.* **160**, 302-320 (2015). Archived as arXiv:math/1408.6714 [math.PR].
- [12] K. Kremer, J. W. Lyklema, Indefinitely growing self-avoiding walk. *Phys. Rev. Lett.* **54**, 267 (1985).

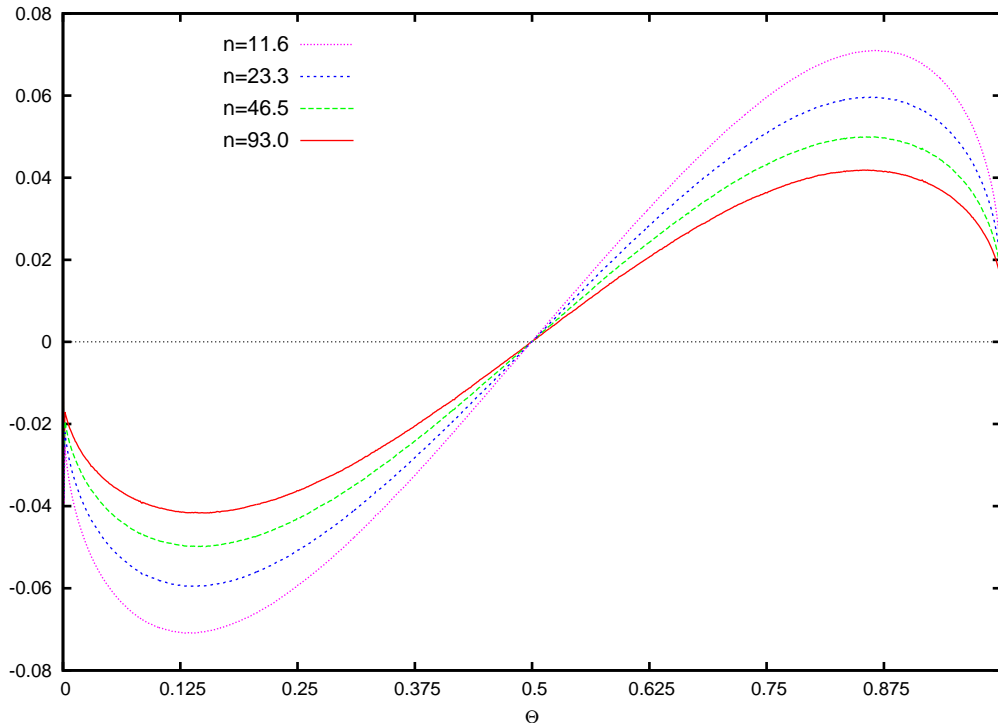


Figure 17: The difference between the percolation explorer and  $SLE_6$  pass right functions for the slit plane when the lattice spacing  $\delta$  is kept fixed and the length  $n$  of the percolation explorer is varied.

- [13] G. Lawler, *Conformally Invariant Processes in the Plane*. American Mathematical Society (2005).
- [14] G.F. Lawler, O. Schramm, and W. Werner, On the scaling limit of planar self-avoiding walk, *Fractal Geometry and Applications: a Jubilee of Benoit Mandelbrot, Part 2*, 339, *Proc. Sympos. Pure Math. 72*, Amer. Math. Soc., Providence, RI, 2004. Archived as arXiv:math/0204277v2 [math.PR].
- [15] G. Lawler, O. Schramm, W. Werner, Conformal Invariance of Planar Loop-Erased Random Walks and Uniform Spanning Trees. *Ann. Probab.* **32**, 939–995, (2004). Archived as arXiv:math/0112234 [math.PR].
- [16] N. Madras and G. Slade, *The Self-Avoiding Walk*. Birkhäuser (1996).
- [17] A. Malakis, Self-avoiding walks on oriented square lattices. *J. Phys. A.* **8** 1885–1898 (1975).
- [18] O. Schramm, A percolation formula. *Electron. Comm. Probab.* **6**, 115–120 (2001). Archived as arXiv:math/0107096.

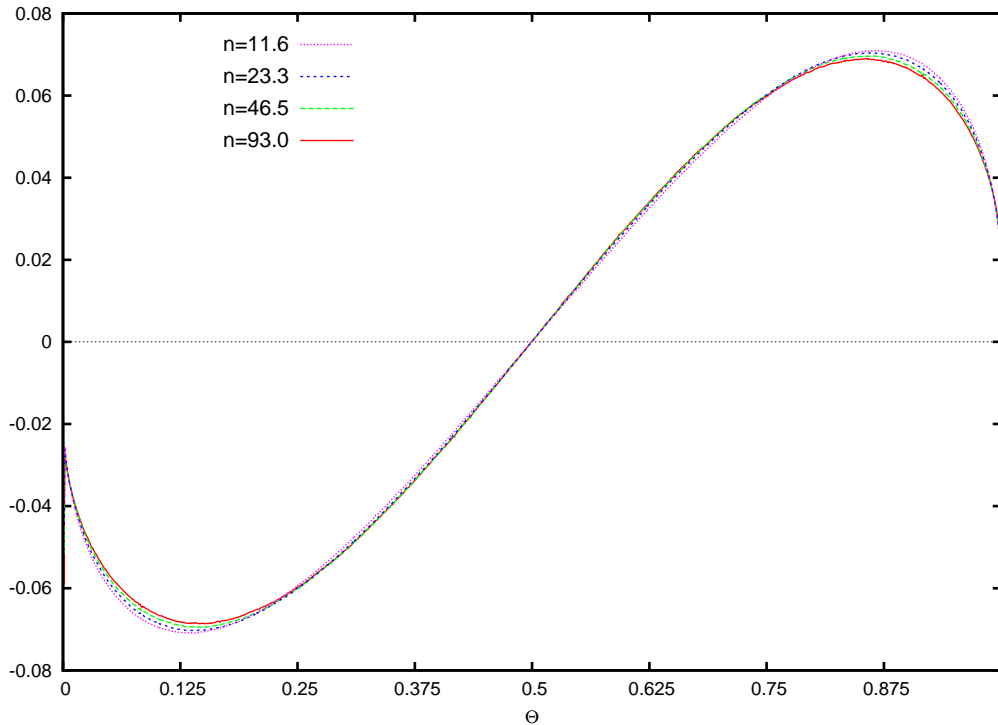


Figure 18: The same differences for the percolation explorer shown in the previous plot are replotted but multiplied by a factor proportional to  $n^p$  with  $p = 0.24$ .

- [19] S. Smirnov, Critical percolation in the plane: Conformal invariance, Cardy's formula, scaling limits. *C. R. Math. Acad. Sci. Paris* **333**, 239–244 (2001). Archived as arXiv:0909.4499 [math.PR].
- [20] A. Weinrib, S. A. Trugman, A new kinetic walk and percolation perimeters. *Phys. Rev. B* **31**, 2993 (1985).
- [21] W. Werner, Lectures on two-dimensional critical percolation, *Statistical Mechanics (IAS/Park City mathematics series v. 16)*, S. Sheffield, T. Spencer (eds.) (2007). Archived as arXiv:0710.0856 [math.PR]
- [22] R. M. Ziff, P. T. Cummings, G. Stells, Generation of percolation cluster perimeters by a random walk. *J. Phys. A* **17**, 3009 (1984).